Journal of Materials Chemistry A

Accepted Manuscript

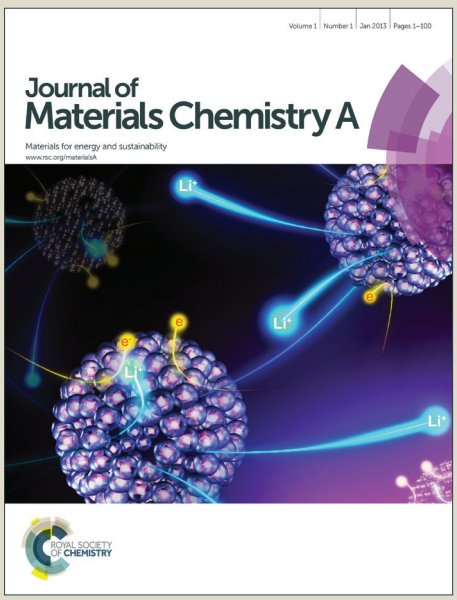

ROYAL SOCIETY OF CHEMISTRY

www.rsc.org/materialsA

Cite this: DOI: 10.1039/c0xx00000x

www.rsc.org/xxxxxx

ARTICLE TYPE

A Water-Soluble Metallophthalocyanine Derivative as Cathode Interlayer for Highly Efficient Polymer Solar Cells

Xiao Cheng, Shuheng Sun, Youchun Chen, YajunGao, Lin Ai, Tao Jia, Fenghong Li* and Yue Wang*

Received (in XXX, XXX) Xth XXXXXXXXX 20XX, Accepted Xth XXXXXXXXX 20XX

DOI: 10.1039/b000000x

A novel organic small molecule water-soluble poly-N-alkylpyridine substitued metallophthalocyanine derivative $VOPc(OPyCH_3I)_8$, namely 2,3,9,10,16,17,23,24-Octakis-[N-methyl-(3-pyridyloxy)] vanadylphthalocyanine iodide (1:8) was synthesized and applied in polymer solar cells (PSCs). Notably, a power conversion efficiency (PCE) of 8.12% for the working area of 2×2 mm^2 and a PCE of 7.23% for the working area of 4×4 mm^2 have been achieved in the PSCs based on this molecule as a cathode interlayer. They are comparable with the higher values of PCE of the PSCs reported currently, indicating that $VOPc(OPyCH_3I)_8$ is a new promising candidate as a good cathode interlayer for highly efficient PSCs.

1. Introduction

Polymer solar cells (PSCs) based on blends comprising conjugated polymers and fullerenes are the subject of considerable investigations because of their potential to enable the fabrication of low-cost devices that convert sunlight into electricity.[1] Currently, the record of power conversion efficiency (PCE) of the bulk-heterojunction (BHJ) PSCs has reached 9%.[2] In order to improve the PCE of BHJ PSCs, significant efforts have been made in terms of new material synthesis,[3] device structure optimization[4] and controlling morphology of active layer.[5] Moreover, the interface of electrode and active layer has as well attracted increased attention to improve device efficiency by minimizing charge collection/extraction barriersand forming ohmic contact between electrode and active layer. Significant improvements in PCE have recently appeared due to an introduction of cathode interlayer between active layer and metal electrode. Many materials such as LiF,[6] metal oxides[7], water-soluble poly(ethylene oxide) (PEO)[8] and alcohol/water-soluble organic or polymeric electrolytes[2a, 2b, 9-11] used as cathode interlayer have successfully enhanced PCE of PSCs. Compared to other cathode interfacial layer materials, advantages of alcohol/water-soluble organic or polymeric materials are apparent in the PSCs due to their simple, vacuum-free and environment-friendly procedure to form film during the device fabrication. Because the alcohol/water solubility of the organic or polymeric materials can avoid intermixing between the active layer and the interlayer, alcohol/water-soluble organic or polymeric molecules are promising cathode interfacial layer materials for all solution processed PSCs. Incorporation of two conjugated polyelectrolytes, poly[3-(6-trimethylammoniumhexyl)thiophene] (P3TMAHT) and poly(9,9-bis(2-ethylhexyl)-fluorene]-*b*-poly[3-(6-trimethylammoniumhexyl)thiophene](PF2/*6*-*b*-P3TMAHT), have improved PSC based on poly[N-9"-heptadecanyl-2,7-carbazole-alt-5,5-(4',7'-di-2-thienyl-2',1',3'-benzothiadiazole)] (PCDTBT):[6,6]-phenyl C71-butyric acidmethyl ester ($PC_{71}BM$) with very good efficiencies, from 5% to >6%.[9a] Recently, Wu and co-workers demonstrated that by incorporating poly[(9,9-dioctyl-2,7-fluorene)-*alt*-(9,9-bis(3′-(*N*,*N*-dimethylamino)propyl)-2,7-fluorene)] (PFN), a typical example among alcohol-soluble polyfluorenes as a cathode interlayer, PSCs have shown simultaneous enhancement in open-circuit voltage (V_{OC}), short-circuit current (J_{SC}) and fill factor (FF). As a result, PCEs of the PSCs based on $PC_{71}BM$ and polymer thieno[3,4-b]-thiophene/benzodithiophene (PTB7) can reach 8.37% in normal architecture[2a] and even up to 9.26% in inverted architecture.[2b]

To be a suitable cathode interlayer for PSC, a material must meet several requirements. Firstly, it has adequate alcohol/water solubility to avoid intermixing between the active layer and the interlayer. Secondly, it can effectively lower the work function (WF) of cathode to facilitate electron extraction from the active layer to electrode while its hole-blocking ability should be good enough as well. Thirdly, it has good electrical conductivity and good film formation property. Finally, it benefits the contact and interfacial compatibility with the active layer. Up to now, the reported organic/polymer cathode interlayers, which could efficiently improve the PCE of PSCs, are very limited. Actually, most of alcohol/water soluble organic cathode interlayers have been designed and synthesized based on fluorine unit with alcohol/water soluble groups.[2a-b,9] In addition, some 3-(6-alcohol/water soluble polymers based on trimethylammoniumhexyl)thiophene have been used as cathode interlayers to construct high efficient polymer solar cells.[10] So far, most of cathode interlayers were formed by polymers. Small organic molecule based cathode interlayers were rare.[11] Compared to polymers, the small molecules have the advantages of well-defined structures, high-purity without batch-to-batch variation and easy modification.[12]

In recent years, metallophthalocyanines have become a hot research topic in the field of organic thin-film transistors (OTFTs) and organic solar cells (OSCs) due to their easy synthesis and adjustable physical properties, high field-effect mobility, intense absorption in the near-infrared (NIR) region and extraordinary thermal and photochemical stability.[13] Generally, metallophthalocyanines are investigated as donor in small molecule solar cells.[13b,13c] However, no researches focus on metallophthalocyanines as a cathode interlayer in PSCs. It is well known that phthalocyanine based molecules are of easy modification, large conjugated π-system, and outstanding stability. Therefore, we select poly-N-alkylpyridine phthalocyanine derivatives as target molecules first. In this study, we synthesized an organic small molecule $VOPc(OPyCH_3I)_8$ named 2,3,9,10,16,17,23,24-Octakis-[N-methyl-(3-pyridyloxy)] vanadylphthalocyanine iodide (1:8) (Scheme 1). The neutral 2,3,9,10,16,17,23,24-Octakis(3-pyridyloxy) vanadyl phthalocyanine ($VOPc(OPy)_8$) could be synthesized directly by the reaction between 4,5-bis(3-pyridinyloxl)phthalonitrile and vanadium (III) trichloride. The purification of $VOPc(OPy)_8$ was very easy by recrystallization and column chromatography due to its good solubility in common organic solvents such as dichloromethane, tetrahydrofuran et al. Methylation of $VOPc(OPy)_8$ with CH_3I resulted in the water soluble vanadyl phthalocyanine ($VOPc(OPyCH_3I)_8$) (Scheme 1), which makes it a potential eco-friendly cathode interlayer in PSCs.

2. Experimental section

2.1 synthesis and characterization

All starting materials were purchased from Aldrich Chemical Co. and used without further purification. The solvents for syntheses were common commercial grade and were used as received. 4,5-Bis(3-pyridinyloxl)phthalonitrile was synthesized according to the reported literature.[14] IR spectra were recorded on a Bruker VERTEX 80v spectrometer. NMR spectra were recorded on a Bruker AVANCE 500 MHz spectrometer with tetramethylsilane as the internal standard. MALDI-TOF mass spectra were recorded on Kratos AXIMA-CFR Kompact MALDI Mass Spectrometer with anthracene-1,8,9-triol as the matrix. Element analyses were performed on a FlashEA1112 spectrometer.

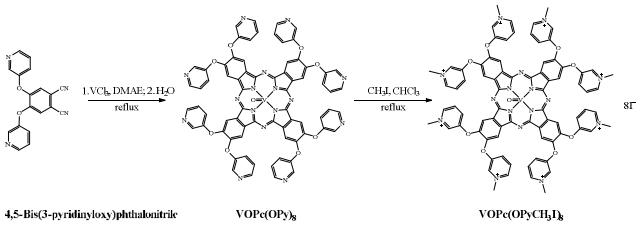

Scheme 1 Synthesis of $VOPc(OPyCH_3I)_8$.

2,3,9,10,16,17,23,24-Octakis(3-pyridyloxy) vanadyl phthalocyanine ($VOPc(OPy)_8$): Under nitrogen, 4,5-Bis(3-pyridinyloxl)phthalonitrile (0.75 g, 2.4 mmol) and VCl_3 (0.19 g, 1.2 mmol) in 4.0 ml dimethylaminoethanol (DMAE) were heated at reflux for 24 h. The reaction proceeded by changing color of the mixture from brown to green. Then 10.0 ml H_2O was added and the mixture was heated at reflux for 8 h accompanying the formation of green precipitate. After cooling to room temperature, the precipitate was filterd and purified by flash column chromatography (silica gel, dichloromethane/methanol: 50/1) to give the pure $VOPc(OPy)_8$ as a green solid. Yield: 53% (0.42 g). IR (υ_{max}/cm^{-1}) (KBr): 705, 752, 802, 863, 894, 1003 (V=O), 1030, 1084 (C-N), 1188, 1212, 1278, 1334, 1404, 1423, 1454, 1475, 1501, 1574, 1613 (C=C ring), 3036(Ar–H). ^1H NMR (500 MHz, CD2Cl2, δ): 7.38 (br, 10H), 7.65 (br, 10H), 8.47 (br, 10H), 8.76 (br, 10H). MS *m/z*: 1323.14 $[M]^+$ (calcd:1323.26), Anal. Found (calcd) for $C_{72}H_{40}N_{16}O_9V$: C 64.96 (65.31), H 3.08 (3.04), N 17.09 (16.92).

2,3,9,10,16,17,23,24-Octakis-[N-methyl-(3-pyridyloxy)] vanadylphthalocyanine, iodide (1:8) ($VOPc(OPyCH_3I)_8$): To a rapidly stirred solution of $VOPc(OPy)_8$ (0.26 g, 0.2 mol) in $CHCl_3$, CH_3I (0.43 g, 3.0 mol) was added and the mixture was heated at reflux for 8 h accompanying the formation of dark green precipitate. After cooling to room temperature, the precipitate was filterd, washed with $CHCl_3$ and dried in vacuo to give the pure $VOPc(OPyCH_3I)_8$. Yield: 98% (0.48 g). IR (υ_{max}/cm^{-1}) (KBr): 751, 830, 880, 954, 1002 (V=O), 1041, 1084 (C-N), 1173, 1280, 1334, 1406, 1451, 1500, 1581, 1612 (C=C ring), 1630 2932-2990 (Aliph. C–H). ^1H NMR (500 MHz, D_2O, δ): 8.77 (br, 40H), 4.56 (d, J = 40 Hz, 24H).MALDI-TOF MS*m/z*: 1338.37$[M-8I-7CH_3]^+$ (calcd: 1338.28), Anal. Found (calcd) for $C_{80}H_{64}I_8N_{16}O_9V$: C 38.88 (39.06), H 2.82 (2.62), N 9.17 (9.11).

2.2 Device fabrication and characterization

Fabrication of polymer solar cells and electron-only devices: PTB7 and PFN were purchased from 1-material Inc. $PC_{71}BM$ was purchased from American Dye Source. All materials were used as received. The blend ratio of PTB7:$PC_{71}BM$ is 1:1.5 by weight and the active layer was spin-casted from mixed solvent of chlorobenzene/1,8-diiodoctane. PFN was dissolved in methanol under the presence of small amount of acetic acid. $VOPc(OPyCH_3I)_8$ was dissolved in water under the presence of 0.6% acetic acid. Firstly PEDOT:PSS (Baytron PVP Al 4083) was spin-coated onto a cleaned ITO and annealed in air at 140°C for 10min. Secondly, blend films of PTB7:$PC_{71}BM$ were spin-casted from solution on PEDOT:PSS and then dried in vacuum. For **Device I**, 100 nm Al was directly vacuum-deposited on the activelayer. For **Device II**, 0.6% acetic acid treatment was carried out by spin-coating water with 0.6% acetic acid on the top of the active layer and then Al was evaporated as a cathode. For **Device III** and **IV**, ~5 nm PFN and $VOPc(OPyCH_3I)_8$ were deposited on the active layer by spin-coating respectively and then Al was evaporated as a cathode. To fabricate electron-only devices, Al was vacuum-deposited on cleaned ITO as an anode. Then same procedures with the fabrication of polymer solar cells described above were followed to complete counterparts (**Device V**, **VI**, **VII** and **VIII**).

Characterization and measurement: Current density-voltage (J-V) characteristics of the devices were measured under N_2 atmosphere in the glove box by using a Keithley 2400 under illumination and in the dark. Solar cell performance was tested under 1 sun, AM 1.5G full spectrum solar simulator (Photo Emission Tech., Inc., model #SS50AAA-GB) with an irradiation intensity of 100 mW/cm^2 calibrated with a standard silicon photovoltaic traced to the National institute of metrology, China.

External quantum efficiency (EQE) spectra were measured using Q Test Station 2000 (Crowntech Inc. USA) at room temperature in air. In addition, the static contact angles of the as-prepared surfaces were measured with a commercial contact angle system (DataPhysics, OCA 20) at ambient temperature using a 4 μl water droplet as the indicator. AFM images were measured by the S II Nanonaviprobe station 300HV by tapping-mode.

3. Results and discussion

In order to highlight the function of the novel small molecule $VOPc(OPyCH_3I)_8$ as a cathode interlayer comparable to PFN in the PSCs, we prepared a set of devices with various cathodes having a working areas of 4×4 mm^2 as follows.

Device I: [ITO/PEDOT:PSS/PTB7:$PC_{71}BM$/Al]

Device II: [ITO/PEDOT:PSS/PTB7:$PC_{71}BM$/0.6% acetic acid/Al]

Device III: [ITO/PEDOT:PSS/PTB7:$PC_{71}BM$/PFN/Al]

Device IV:

[ITO/PEDOT:PSS/PTB7:$PC_{71}BM$/$VOPc(OPyCH_3I)_8$/Al]

For comparison, the two control devices (namely **Device I** and **DeviceII**) have been fabricated. In **Device I**, Al was directly deposited on the active layer. In **Device II**, Al was deposited on the active layer treated by the solution of 0.6% acetic acid in water, which is the solvent of $VOPc(OPyCH_3I)_8$. It aims to figure out that main contribution of enhanced PSC performance is not from the solvent of $VOPc(OPyCH_3I)_8$ but from $VOPc(OPyCH_3I)_8$ itself.

Table 1. The performances of PTB7:$PC_{71}BM$ PSCs (working area = 4×4 mm^2) with the various cathodes.

Device	Voc (V)	Jsc (mA/cm^2)	FF (%)	PCE(%) Max	PCE(%) Aver	R_s (Ωcm^2)	R_{sh} (Ωcm^2)	Rectification ratio
I	0.675	14.00	50	4.77	4.72	15.8	588	251
II	0.699	13.83	54	5.18	5.15	14.9	526	7546
III	0.755	15.23	61	6.99	6.86	10.2	1003	24827
IV	0.765	15.31	62	7.23	6.95	9.6	1100	13513

Figure 1 shows the current density versus voltage (J-V) characteristics of the above four PSCs under AM 1.5G illumination at 100 $mW{\cdot}cm^{-2}$ (a) and in the dark (b), and the external quantum efficiency (EQE) (c). Table 1 presents a summary of open circuit (Voc), short circuit (Jsc), fill factor (FF), power conversion efficiency (PCE), series resistance (Rs) and shunt resistance (Rsh) derived from J-V characteristics under illumination, and rectification ratio derived from J-V characteristics in the dark.

Under illumination, devices with $VOPc(OPyCH_3I)_8$/Al (**Device IV**) and PFN/Al (**Device III**) as cathodes show a Voc of 0.765 V and 0.755 V respectively, which are higher than the control devices with (Voc = 0.699V, **Device II**) and without (Voc = 0.675 V, **Device I**) 0.6% acetic acid treatment. The increase in Voc can be mainly attributed to the reduced work function (WF) of Al cathode. Ultraviolet photoemission spectroscopic (UPS) measurements were carried out with monohromatized HeI radiation at 21.2 eV. Figure 2 shows UPS spectra of bare Al, Al treated by 0.6% acetic acid in the water, Al covered by 5 nm PFN and Al covered by 5 nm $VOPc(OPyCH_3I)_8$ in the secondary electron cutoff region. WF is defined by secondary electron cutoff. As a result, the WF values are 4.2 eV for bare Al, 3.5 eV for Al/0.6% acetic acid, 3.3 eV for Al/PFN, and 3.3 eV for Al/$VOPc(OPyCH_3I)_8$, respectively.

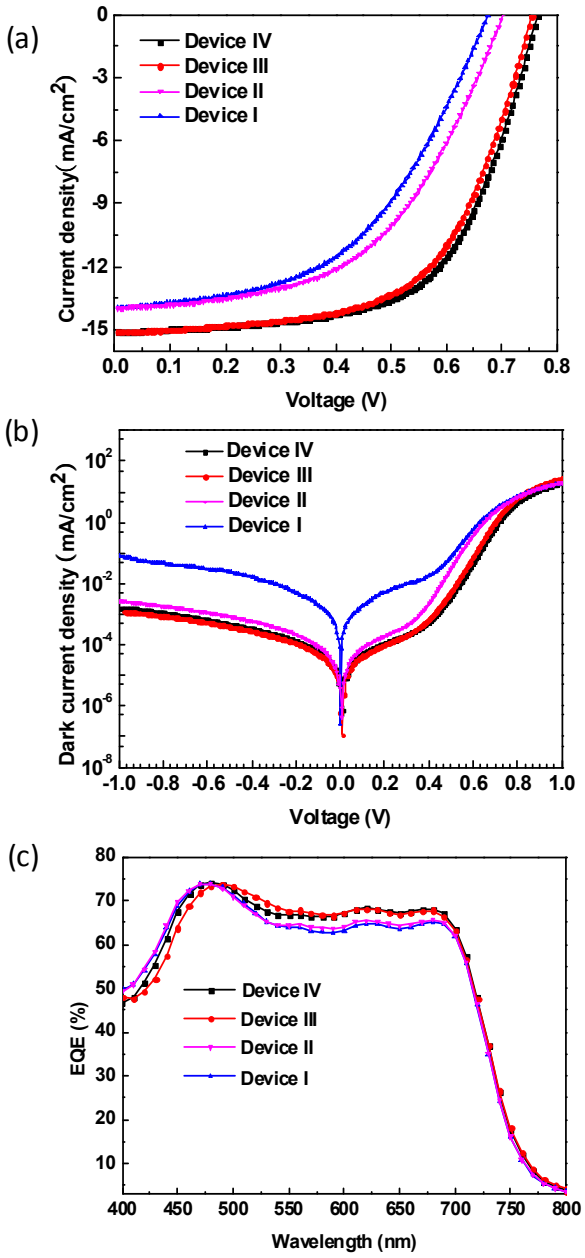

Figure 1. The effect of different cathodes on PSC performance. (a) Current density versus voltage (J-V) characteristics of devices with $VOPc(OPyCH_3I)_8$(black squares), PFN (red circles) as a cathode interlayer, and with (magenta down-triangles) and without (blue up-triangles) 0.6% acetic acid treatment at the surface of active layer under 100 mW/cm^2 AM 1.5G illumination. (b) J-V characteristics of the above four devices in the dark. (c) EQE spectra of the above four devices.

UPS measurements demonstrated that the WF of Al was decreased due to the treatment of 0.6% acetic acid and coverage of PFN or $VOPc(OPyCH_3I)_8$ on the Al surface. More importantly,

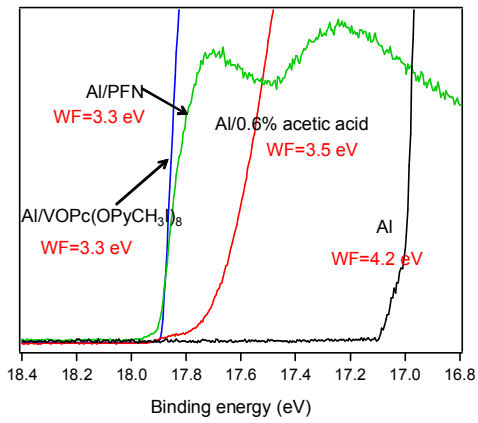

Figure 2. UPS spectra of bare Al, Al treated by 0.6% acetic acid in the water, Al covered by 5 nm PFN and Al covered by 5 nm $VOPc(OPyCH_3I)_8$ in the secondary electron cutoff region. Work function (WF) is defined by secondary electron cutoff.

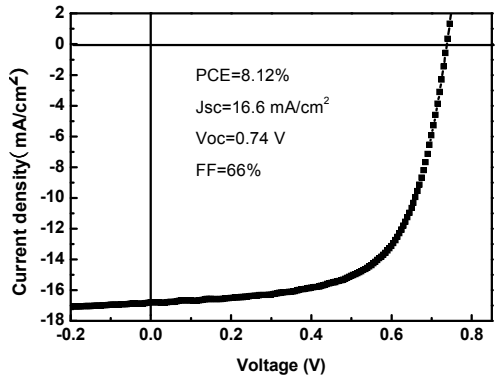

Figure 3. J-V characteristics of device (ITO/PEDOT:PSS/PTB7:$PC_{71}BM$/$VOPc(OPyCH_3I)_8$/Al) with a working area of 2×2 mm^2

PCE of **Device IV** (7.23%) is much higher than **Devices I** (4.77%) and **II** (5.18%) due to simultaneous enhancement in Voc, Jsc and FF as presented in Table 1. It is clear that introduction of $VOPc(OPyCH_3I)_8$ between active layer and Al cathode results in the improved PCE and the contribution from the solvent (0.6% acetic acid) to the PSCs performanceis relatively smaller even though 0.6% acetic acid treatment improve Voc and FF as well. Moreover, PCE of **Device IV** (7.23%) is also higher than one of **Device III** (6.99%) with PFN as a cathode interlayer. When PFN was replaced by $VOPc(OPyCH_3I)_8$ as a cathode interlayer, Voc increased from 0.755 V to 0.764, Jsc from 15.23 mA/cm^2 to 15.31 mA/cm^2, and FF from 61% to 62% as shown in Figure 1a and data in the Table 1. We surmise at this point that incorporating $VOPc(OPyCH_3I)_8$ as a cathode interlayer can more effectively enhance PCE of PSCs than PFN in this study. It should be noted that the working area of all devices shown in Figure 1 is 4×4 mm^2. When device working area decreases from 4×4 mm^2 to 2×2 mm^2, PCE of the PSCs with $VOPc(OPyCH_3I)_8$ as a cathode interlayer can reach 8.12% due to Jsc of 16.6 mA/cm, Voc of 0.74 V and FF of 66% as shown in Figure 3.

Table 1 also presents series resistances (R_s) and shunt resistances (R_{sh}) of devices obtained from the slops of J-V curves at V_{OC} and J_{SC}, respectively (Figuer 1a). The R_s and R_{sh} of only-Al device (**Device I**) is 15.8 Ω cm^2 and 588 Ω cm^2, respectively. The R_s (14.9 Ω cm^2) and R_{sh} (526 Ω cm^2) of device based on active layer treated by 0.6% acetic acid (**Device II**) are more or less similar to ones of **Device I**. However a decrease of R_s and an increase of R_{sh} are apparent when PFN or $VOPc(OPyCH_3I)_8$ was utilized as a cathode interlayer. For **Device III** with PFN, the R_s decreases to 10.2 Ω cm^2 and the R_{sh} increases to 1003 Ω cm^2. For **Device IV** with $VOPc(OPyCH_3I)_8$, the R_s further decreases to 9.6 Ω cm^2 and the R_{sh} increases to 1100 Ω cm^2. The increase of J_{sc} of the devices with a cathode interlayer is attributed to the resistance changes. The excellent diode quality of **Devices III** and **IV** with very low leakage current and high rectification ratio is clearly proved in the dark J-V characteristics.

In the dark, both **Devices III** and **IV** exhibit a turn-on voltage around 0.80 V while it is around 0.70 V for the control devices as shown in Figure 1b. It indicates that the built-in voltage (V_{bi}) (here considered as flat-band condition) of the device increases around 100 mV when incorporating PFN or $VOPc(OPyCH_3I)_8$ as a cathode interlayer. Because V_{bi} influences the internal electric field in polymer BHJ solar cells and gives the upper limit for the Voc provided that the WF difference of electrodes is larger than the donor HOMO-acceptor LUMO offset of the BHJ. Thus the increase of V_{bi} may be responsible for the increase in Voc in the **Devices III** and **IV** with PFN and $VOPc(OPyCH_3I)_8$ as a cathode interlayer, respectively. In addition, the electrical leakage for the devices with a cathode interlayer is suppressed because the **Devices III** and **IV** have higher rectification ratios at ±1 V than the control devices. As listed in Table 1, the rectification ratios of **Devices III** and **IV** are 24827 and 13513, respectively, while one of **Device I** (only Al) is only 251 and one of **Device II** (0.6% acetic acid treatment) is 7546. **Device II** has a lower leakage current and higher rectification ratio than **Device I**, indicating that the solvent treatment can improve the diode quality and FF value.

The external quantum efficiency (EQE) spectra of various devices from 400 nm to 800 nm are shown in Figure 1c. The improved PCEs of **Devices III** and **IV** are consistent with higher EQE values, which approach 75% around 490 nm. The Jsc values calculated from integration of the EQE spectra are 15.12 mA/cm^2 for **Device IV** and 14.72 mA/cm^2 for **Device III**, which are in good agreement with the Jsc=15.31 mA/cm^2 of **Device IV** (ca. 1.2% error) and the Jsc=15.23 mA/cm^2 of **Device III** (ca. 3.3% error) obtained from J-V characteristics under illumination.

Compared to the control devices, **Device III** with PFN and **Device IV** with $VOPc(OPyCH_3I)_8$ show higher FF values as listed in Table 1. It implies that introduction of cathode interlayer (PFN or $VOPc(OPyCH_3I)_8$) effectively improved charge transport ability, in particular for electron transport. In order to confirm that electron transport of PSCs is enhanced when a cathode interlayer is used, we carried out J-V measurements of four electron-only devices, which are **Device V**(ITO/Al/PTB7:$PC_{71}BM$/Al), **Device VI** (ITO/Al/PTB7:$PC_{71}BM$/0.6% acetic acid/Al), **DeviceVII** (ITO/Al/PTB7:$PC_{71}BM$/PFN/Al) and **Device VIII** (ITO/Al/PTB7:$PC_{71}BM$/$VOPc(OPyCH_3I)_8$/Al). As shown in Figure 4, current densities of devices with a cathode interlayer (**Devices VII** and **VIII**) are obviously higher than ones of devices without a cathode interlayer (**Devices V** and **VI**). It means that the devices with a cathode interlayer have better electron collection and transport properties. More importantly the electron

mobility can be measured in the space charge limited current (SCLC) regime as described by

$$J=9\varepsilon_0\varepsilon_r\mu V^2/8L^3 \quad (1)$$

where ε_0 is the permittivity of free space, ε_r is the dielectric constant of the active layer, μ_e is the electron mobility, V is the voltage drop across the device, L is the active layer thickness. The above equation holds if the mobility is field independent. Figure 4b presents our $J^{0.5}$-V analysis for the four electron-only devices (**Device V-VIII**), where V_r (the voltage drop due to contact resistance and series resistance across the electrodes) and V_{bi} (the built-in voltage due to the difference in work function of the two electrodes at both sides of active layer) are subtracted from experimental applied voltage.[2a, 15] ε_r is assumed to be 3.9 in our analysis.[2a] A straight line going through the origin of $J^{0.5}$-V curves for the four devices signifies that the mobility is field independent at field up to 2×10^5 V/cm. The field independent mobilities calculated from Eq. (1) are 2.7×10^{-5} cm^2/V s for **Device V**, 3.6×10^{-5} cm^2/V s for **Device VI**, 4.6×10^{-4} cm^2/V s for **Device VII** and 7.1×10^{-4} cm^2/V s for **Device VIII** (Details and parameters in Table S1). For **Devices I-VIII**, the thickness of active layer is 120 nm. The electron-only devices, in which the thickness of active layer is 170 nm, displayed similar mobility feature (see Table S1). It is apparent that the incorporation of a cathode interlayer increases the electron mobility up to one order of magnitude and sequence of the electron transport capability for the four electron-only devices is **Device VIII>Device VII>Device VI>Device V**. It is in agreement with the increasing trend of FF in PSCs as list in Table 1. At the same time, in order to prove that introducing a cathode interlayer facilitates a balance of charge carrier transport, we also carried out the J-V characteristics of hole-only devices (J-V curves are shown in Figure S2), which are Device IX (ITO/PEDOT:PSS/PTB7:PC_{71}BM/MnO_3/Al), Device X (ITO/PEDOT:PSS/PTB7:PC_{71}BM/0.6% acetic acid /MnO_3/Al), Device XI (ITO/PEDOT:PSS/PTB7:PC_{71}BM/PFN/MnO_3/Al) and Device XII (ITO/PEDOT:PSS/PTB7:PC_{71}BM/ $VOPc(OPyCH_3I)_8$/MnO_3/Al). According to Eq. (1), hole mobilities in Devices **IX-XII** are 3.29×10^{-4} cm^2/V s, 4.32×10^{-4} cm^2/V s, 7.28×10^{-4} cm^2/V s and 6.82×10^{-4} cm^2/V s, respectively. It is apparent that a perfect mobility balance of hole and electron has been achieved when $VOPc(OPyCH_3I)_8$ is used as a cathode interlayer.

Figure 5 shows the surface morphologies obtained by atomic force microscopy (AFM) measured at ambient. The surface of PTB7:PC_{71}BM BHJ film is smooth with a root-mean-square (RMS) roughness of 2.65 nm (Figure 5a). However the surface of PTB7:PC_{71}BM film treated by 0.6% acetic acid in water become smoother due to a RMS roughness of 1.34 nm and remained homogeneous as shown in Figure 5b. It indicates that no obvious reconstruction of the surface of PTB7:PC_{71}BM blends after 0.6% acetic acid treatment. These observations are similar to the PCDTBT:PC_{71}BM blends treated by methanol[10a] and slightly different from the PTB7:PC_{71}BM blends treated by methanol, which did not cause an observable change on morphology and roughness of film.[16] Therefore the improvement of Voc and FF in the **Deice II** with 0.6% acetic acid treatment is hardly related with the change on morphology. When an ultrathin PFN film like in the **Device III** is spin-coated on PTB7:PC_{71}BM blends, the RMS roughness of the surface becomes 3.41 nm (Figure 5c), indicating that PFN has a good property of film forming on PTB7:PC_{71}BM blends. However, $VOPc(OPyCH_3I)_8$-treated surface of PTB7:PC_{71}BM blend shows a much rougher morphology with RMS value of 9.34 nm. Notably, there are some visible islands distributed over the surface. The formation mechanism of the islands may be the self-aggregation of $VOPc(OPyCH_3I)_8$ itself. This is probably due to its high polarity and adverse wettability of $VOPc(OPyCH_3I)_8$ aqueous solution on the hydrophobic active layer. Moreover we found that RMS roughness of $VOPc(OPyCH_3I)_8$-treated surface of PTB7:PC_{71}BM increased with the development of time. As rough morphology is usually adverse for the device performance, the AFM result implies the great potential of VOPc as cathode interlayer in PSCs.

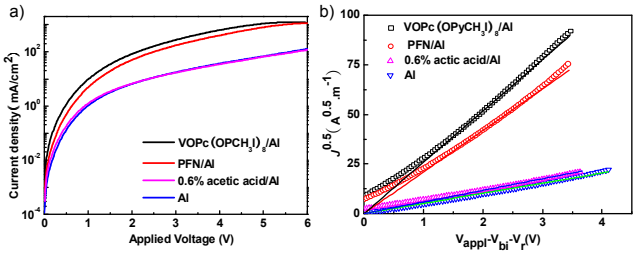

Figure 4. (a) Experimental dark current density-applied voltage (*J*-V) characteristics of electron-only devices with $VOPc(OPyCH_3I)_8$ (black line), PFN (red line) as a cathode interlayer, and with (magenta line) and without (blue line) 0.6% acetic acid treatment at the surface of active layer. (b) $J^{0.5}$ vs. V_{appl}-V_{bi}-V_r plots for the same elelctron-only devices with in (a).

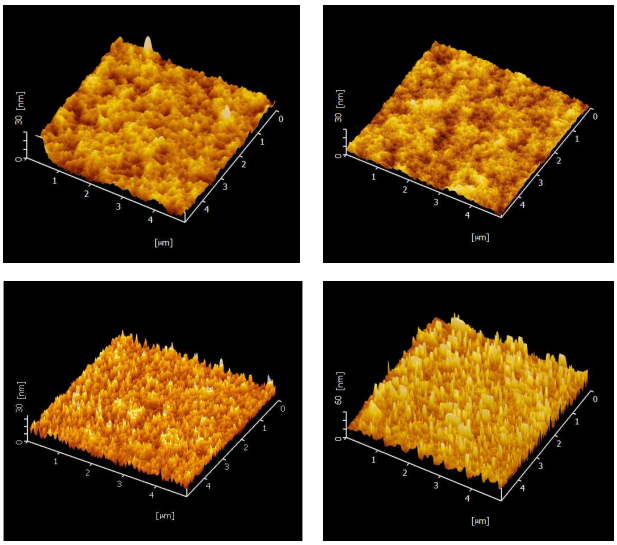

Figure 5. AFM images of (a) PTB7:PCBM BHJ film, (b) PTB7:PC_{71}BM BHJ film treated by 0.6% acetic acid in water, (c) PFN on PTB7:PC_{71}BMBHJ film and (d) $VOPc(OPyCH_3I)_8$ on PTB7:PC_{71}BM BHJ film.

In order to check the surface polarity, measurements of the water contact angle (θ) were performed on the surface of PTB7:PC_{71}BM, PTB7:PC_{71}BM/0.6% acetic acid, PTB7:PC_{71}BM/PFN and PTB7:PC_{71}BM/$VOPc(OPyCH_3I)_8$. The images were collected with a digital camera. As shown in Figure 6a and b, the surfaces of PTB7:PC_{71}BM and PTB7: PC_{71}BM treated by 0.6% acetic acid are largely hydrophobic, the water

contact angles of which are 101.7° and 100.8° respectively. It indicates that 0.6% acetic acid treatment only slightly changed the surface polarity of PTB7: $PC_{71}BM$. However when PFN was spin-coated on PTB7:$PC_{71}BM$ film, the surface becomes slightly hydrophilic (θ≈82.7°, as shown in Figure 6c). In contrast, the surface of PTB7:$PC_{71}BM$/$VOPc(OPyCH_3I)_8$ is hydrophilic due to θ≈50.3° presented in Figure 6d, indicating accumulation of ionic component at the topmost organic surface and a dipole layer exists on the surface. The $VOPc(OPyCH_3I)_8$ interlayer induced the decrease of the WF of Al also demonstrated the formation of interfacial dipole layer. The detail microscopic mechanism of the interfacial dipole remains unclear so far. However, the extensively accepted viewpoint is that the interfacial dipole can improve the charge transport, extraction and Voc of solar cell.[2a-b,8-11] Therefore, PCE increase should be mainly attributed to the formation of interfacial dipole layer in the solar cell. It is worth to note that other mechanism including n-type doping of contacted $PC_{71}BM$ by anions of $VOPc(OPyCH_3I)_8$,[17] the integer charge-transfer mode, electron cloud push-back effects and so on cannot be ruled out now. [18]

Four kinds of solvent conditions (methanol, methanol + 0.6% acetic acid, water, water + 0.6% acetic acid) have been employed to dissolve $VOPc(OPyCH_3I)_8$ for the interlay preparation. As a result, device performance was best when 0.6% acetic acid was added into water as a solvent of $VOPc(OPyCH_3I)_8$. It was demonstrated that the introduction of small amount of acetic acid could improve the polymer solar cell performance.[2a-b,9c] So far, precise mechanism for the result in this study remains unclear. We suppose that an addition of a small amount of acetic acid may give rise to partial protonation of $VOPc(OPyCH_3I)_8$ molecules that may consequently influence the microstructure of interlayer.[19] On the other hand, the residual trace of acetic acid in the interlayer may react with aluminumcathode, which should affect the property of interlayer.

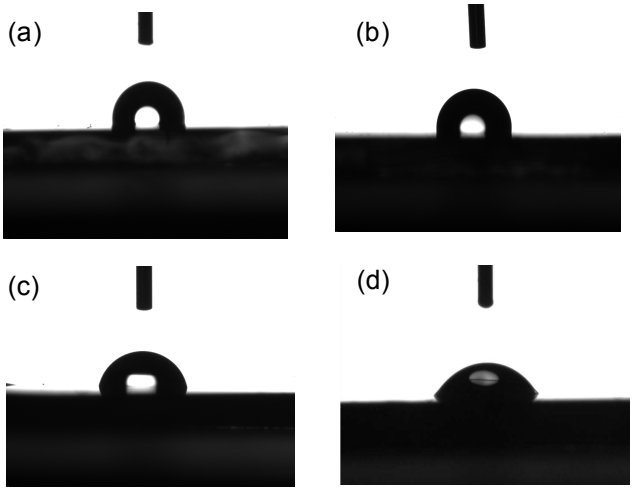

Figure 6. Photos of water droplets on the surfaces of (a) PTB7:$PC_{71}BM$ BHJ film, (b) PTB7:$PC_{71}BM$ BHJ film treated by 0.6% acetic acid in water, (c) PFN on PTB7:$PC_{71}BM$ BHJ film and (d) $VOPc(OPyCH_3I)_8$ on PTB7:$PC_{71}BM$ BHJ film.

4. Conclusions

In conclusion, a novel cathode interlayer, $VOPc(OPyCH_3I)_8$, has been synthesized and successfully utilized in the PSCs based on PTB7:$PC_{71}BM$ as an active layer. Compared to the two control devices, a simultaneous enhancement in V_{OC}, J_{SC} and FF of the PSC with $VOPc(OPyCH_3I)_8$ as a cathode interlayer has been observed. As a result, a PCE of 8.12% for the working areas of 2×2 mm^2 and a PCE of 7.23% for the working areas of 4×4 mm^2 have been achieved. They are comparable with the higher values of PCE of the PSCs reported currently. It indicates that $VOPc(OPyCH_3I)_8$ is a new promising candidate as a good cathode interlayer for highly efficient PSCs. Recently, we have demonstrated that not only phthalocyanine but also other classes of organic conjugated molecules modified with poly-N-alkylpyridine anions can be employed as cathode interlayer to significantly improve the performance of PSC. These results will be reported elsewhere. Therefore, the modification of organic molecules with poly-N-alkylpyridine anions should be an efficient strategy for the design and synthesis of high-performance alcohol/water soluble organic cathode interlayers that can be employed to fabricate high performance polymer solar cells.

Acknowledgements

This work was supported by grants fromthe National Basic Research Program of China (2014CB643500) and the Natural Science Foundation of China (51273077and 51173065).

Notes and references

State Key Laboratory of Supramolecular Structure and Materials, Jilin University, Qianjin Avenue,Changchun, 130012, P. R. China . Fax: XX XXXX XXXX; Tel: XX XXXX XXXX; E-mail: jhli@jlu.edu.cn; yuewang@jlu.edu.cn

† Electronic Supplementary Information (ESI) available: [details of J-V characteristics of electron-only devices]. See DOI: 10.1039/b000000x/

‡ X. Cheng and S. Sun contributed equally to this work.

1 a) J. Peet, J. Y. Kim, N. E. Coates, W. L. Ma, D. Moses, A. J. Heeger & G. C. Bazan, *Nat. Mater* 2007, **6**, 497; b) J. Y. Kim, K. Lee, N. E. Coates, D. Moses, T.-Q. Nguyen, M. Dante, A. J. Heeger, *Science* 2007, **317**, 222 ; c) S. H. Park, A. Roy, S. Beaupré, S. Cho, N. Coates, J. S. Moon, D. Moses, M. Leclerc, K. Lee, A. J. Heeger, *Nat. Photonics* 2009, **3**, 297; d) G. Li, R. Zhu, Y. Yang, *Nat. Photonics* 2012, **6**, 153; e) L. Dou, J. You, J. Yang, C.-C. Chen, Y. He, S. Murase, T. Moriarty, K. Emery, G. Li, Y. Yang, *Nat. Photonics* 2012, **6**, 180; f) Y. Li, *Acc. Chem. Res*. 2012, **45**, 723; g) J. Chen, Y. Cao, *Acc. Chem. Res*. 2009, **42**, 1709.

2 a) Z. He , C. Zhong , S. Su , M. Xu , H. Wu, Y. Cao , *Nat. Photonics* 2012, **6**, 591; b) Z. He, C. Zhong, X Huang, W.-Y. Wong, H. Wu, L. Chen, S. Su, Y. Cao, *Adv. Mater.* 2011, **23**, 4636; c) S.-H. Liao, H.-J. Jhou, Y.-S. Cheng and S.-A. Chen, Adv. Mater., 2013, **25**, 4766; d) X. Li, W. C. H. Choy, L. Huo, F. Xie, W. E. I. Sha, B. Ding, X. Guo, Y. Li, J. Hou, J. You, Y. Yang, *Adv. Mater.* 2012, **24**, 3046; e) J. You, X. Li, F. Xie, W. E. I. Sha, J. H. W. Kwong, G. Li, W. C. H. Choy, Y. Yang, *Adv. Energy Mater.* 2012, **2**, 1203; f) M. Zhang, X. Guo, S. Zhang, J. Hou, *Adv. Mater.* 2013, **7**, 118;

3 a) Y. Liang, Z. Xu, J. Xia, S. T. Tsai, Y. Wu, G. Li, C. Ray, L. Yu, *Adv. Mater.* 2010, **22**, E135; b) S. H. Park, A. Roy, S. Beaupré, S. Cho, N. Coates, J. S. Moon, D. Moses, M. Leclerc, K. Lee, A. J. Heeger, *Nat. Photonics* 2009, **3**, 297; c) B. Carsten, F. He, H. J. Son, T. Xu, L. Yu, *Chem. Rev.* 2011, **111**,1493; d) X. Guo, N. Zhou, S. J. Lou, J. Smith, D. B. Tice, J. W. Hennek. R. P. Ortiz, J. T. L. Navarrete, S. Li, J. Strzalka, L. X. Chen, R. P. H. Chang, A. Facchetti, T. J. Marks, *Nat. Photonics* 2013, **7**, 825; e) L. Huo, S. Zhang, X. Guo, F. Xu, Y. Li, J. Hou, *Angew. Chem. Int. Ed*. 2011, **50**, 9697; f) Y. Deng, J. Liu, J. Wang, L. Liu, W. Li, H. Tian, X.

Zhang, Z. Xie, Y. Geng, F. Wang, *Adv. Mater.* 2013, **3**, 471; g) Y. Huang, X. Guo, F. Liu, L. Huo, Y. Chen, T. P. Russell, C. C. Han, Y. Li, J. Hou, *Adv. Mater.* 2012, **24**, 3383; h) Y. Dong, X. Hu, C. Duan, P. Liu, S. Liu, L. Lan, D. Chen, L. Ying, S. Su, X. Gong, F. Huang, Y. Cao, *Adv. Mater.* 2013, **25**, 3683.

4 a) C. Gu, Y. Chen, Z. Zhang, S. Xue, S. Sun, K. Zhang, C. Zhong, H. Zhang, Y. Pan, Y. Lv, Y. Yang, F. Li, S. Zhang, F. Huang, and Y. Ma, *Adv. Mater.* 2013, **25**, 3443; b) C. E. Small, S. Chen, J. Subbiah, C. M. Amb, S.-W. Tsang, T.-H. Lai, J. R. Reynolds, F. So, *Nat. Photonics* **2012**, **6**, 115; c) Y. Sun, J. H. Seo, C. J. Takacs, J. Seifter, A. J. Heeger, *Adv. Mater.* **2011**, **23**, 1679; d) J. You, C.-C.Chen, L. Dou, S. Murase, H.-S. Duan, S. A. Hawks, T. Xu, H. J. Son, L. Yu, G. Li, Y. Yang, *Adv. Mater.* 2012, **24**, 5267; e) H. Kang, S. Hong, J. Lee, K. Lee, *Adv. Mater.* 2012, **24**, 3005; f) J. Liu, S. Shao, G. Fang, B. Meng, Z. Xie, L. Wang, *Adv. Mater.* 2012, **24**, 2774.

5 a) J. Jo, S.-I. Na, S.-S. Kim, T.-W. Lee, Y. Chung, S.-J. Kang, D. Vak, D.-Y. Kim, *Adv. Funct. Mater.* 2009, **19**, 2398.

6 a) C. J. Brabec, S. E. Shaheen, C. Winder, N. S. Sariciftci, P. Denk, *Appl. Phys. Lett*. 2002, **80**, 1288; b) Z. Chen, H. Zhang, Z. Xing, J. Hou, J. Li, H. Wei, W. Tian, B. Yang, *Solar Energy Materials & Solar Cells*, 2013, **109**, 254.

7 a) J. Y. Kim, S. H. Kim, H.-H. Lee, K. Lee, W. Ma, X. Gong, A. J. Heeger, *Adv. Mater*. 2006, **18**, 572; b) S. K. Hau, H.-L. Yip, H. Ma, A. K.-Y. Jen, *Appl. Phys. Lett*. 2008, **93**, 233304; c) Z. Chen, H. Zhang, W. Yu, Z. Li, J. Hou, H. Wei, B. Yang, *Adv. Energy Mater.* 2013, **3**, 433; d) Z. Chen, H. Zhang, Q. Zeng, Y. Wang, D. Xu, L. Wang, H. Wang, B. Yang, *Adv. Energy Mater.* 2014, DOI: 10.1002/aenm.201400235.

8 F. L. Zhang, M. Ceder, O. Inganäs Adv. Mater. 2007, **19**, 1835.

9 a) Z. Tang, L. M. Andersson, Z. George, K. Vandewal, K. Tvingstedt,P. Heriksson, R. Kroon, M. R. Andersson, O. Inganäs, *Adv. Mater.* 2012, **24**, 554;b) S.-H. Oh, S.-I. Na, J. Jo, B. Lim, D. Vak, D.-Y. Kim, *Adv. Funct. Mater*. 2010, **20**, 1977; c) M. Lv, S. Li, J. J. Jasieniak, J. Hou, J. Zhu, Z. Tan, S. E. Watkins, Y. Li, X. Chen, *Adv. Mater.* 2013, **25**, 6889; d) S.-H. Liao, Y.-L. Li, T.-H. Jen, Y.-S. Cheng, S.-A. Chen, *J. Am. Chem. Soc.* 2012, **134**, 14271; e) S. Liu, K. Zhang, J. Lu, J. Zhang, H.-L. Yip, F. Huang, Y. Cao, *J. Am. Chem. Soc.* 2013, **135**, 15326; f) B. H. Lee, I. H. Jung, H. Y. Woo, H.-K. Shim, G. Kim, K. Lee, *Adv. Funct. Mater.* 2014, **24**, 1100; g) Y. Zhao, Z. Xie, C. Qin,Y. Qu, Y. Geng, L. Wang, *Solar Energy Materials & Solar Cells*, 2009, **93**, 604; h) Q. Mei, C. H. Li, X. Gong, H. Lu,E. G. Jin, C. Du, Z. Lu, L. Jiang, X. Y. , C. R. Wang, Z. S. Bo, ACS Appl. Mater. Interfaces, 2013, **5***,* 8076.

10 a) J. H. Seo, A. Gutacker, Y. Sun, H. Wu, F. Huang, Y. Cao, U. Scherf, A. J. Heeger, G. C. Bazan, *J. Am. Chem. Soc*. 2011, **133**, 8416; b) Y.-M. Chang, R. Zhu, E. Richard, C.-C. Chen, G. Li, Y. Yang, *Adv. Funct. Mater.* 2012, **22**, 3284.

11 a) S. S. Li, M. Lei, M. L. Lv, S. E. Watkins, Z. A. Tan, J. Zhu, J. H. Hou, X. W. Chen and Y. F. Li, Adv. Energy Mater., 2013, 3, 1569. b) H. Ye, X. Hu, Z. Jiang, D. Chen, X. Liu, H. Nie, S.J. Su, X. Gong, Y. Cao, *J. Mater. Chem. A* 2013, **1**, 3387; c) X. Li, W. Zhang, Y. Wu, C. Mina, J. Fang, *J. Mater. Chem. A* 2013, 1, 12413;d) C. H. Wu, C. Y. Chin, T. Y. Chen, S. N. Hsieh, C. H. Lee, T. F. Guo, A. K. Y. Jen, Ten-Chin Wen, *J. Mater. Chem. A* 2013, **1**, 2582; e) Z.-G Zhang, B. Qi, Z. Jin, D.Chi, Z. Qi, Y. Li, J. Wang, *Energy Environ. Sci.* 2014, DOI: 10.1039/C4EE00022F; f) M. Vasilopoulou, D. G. Georgiadou, A. M. Douvas, A. Soultati, V. Constantoudis, D. Davazoglou, S. Gardelis, L. C. Palilis, M. Fakis, S. Kennou, T. Lazarides, A. G. Coutsolelos and P. Argitis，*J. Mater. Chem. A* 2014, **2**, 182; g) D. Chen , H. Zhou , M. Liu , W. M. Zhao , S. J. Su , Y. Cao, *Macromol. Rapid Commun.* 2013*,* **34***,* 595.

12 a) J. Zhou, X. Wan, Y. Liu, Y. Zuo, Z. Li, G. He, G. Long, W. Ni, C. Li, X. Su, Y. Chen, *J. Am. Chem. Soc.* 2012, **134**, 16345; b) Y. Liu, Y. M. Yang, C.-C. Chen, Q. Chen, L. Dou, Z. Hong, G. Li, Y. Yang, *Adv. Mater.* 2013, **25**, 4657; c) X. Zhang. Z. Lu, L. Ye, C. Zhan, J. Hou, S. Zhang, B. Jiang, Y. Zhao, J. Huang, S. L. Zhang, Y. Liu, Q. Shi, Y. Liu, J. Yao, *Adv. Mater.* 2013, **25**, 5791; d) K. Lu, J. Yuan, J. Peng, X. Huang, L. Cui, Z. Jiang, H. Q. Wang, W. Ma, *J. Mater. Chem. A* 2013, **1**, 14253.

13 a) S. Dong, H. Tian, D. Song, Z. Yang, D. Yan, Y. Geng, *Chem. Commun.* 2009, 3086; b) A. Foertig, A. Wagenpfahl, T. Gerbich, D. Cheyns, V. Dyakonov, C. Deibel, *Adv. Energy Mater.* 2012, **2**, 1483; c) B. P. Rand, D. Cheyns, K. Vasseur, N. C. Giebink, S. Mothy, Y. Yi, V. Coropceanu, D. Beljonne, J. Cornil, J.-L. Brédas, J. Genoe, *Adv. Funct. Mater.* 2012, **22**, 2987.

14 D. Wöhrle, M. Eskes, K. Shigehara, A. Yamada, *Synthesis* **1993**, 194.

15 a) C. Goh, R. J. Kline, M. D. McGehee, E. N. Kadnikova, J. M. J. Fréchet, *Appl. Phys. Lett*. 2005, **86**, 122110; b) Y. Liang, D. Feng, Y. Wu, S.-T. Tsai, G. Li, C. Ray, L. Yu, *J. Am. Chem. Soc*. 2009, **131**, 7792.

16 H. Zhou, Y. Zhang, J. Seifter, S. D. Collins, C. Luo, G. C. Bazan, T-Q. Nguyen, A. J. Heeger, *Adv. Mater*. 2013, **25**, 1646.

17 C.-Z. Li, C.-C. Chueh, F. Ding, H.-L. Yip, P.-W. Liang, X. Li, A. K.-Y. Jen, *Adv. Mater*. 2013, **25**, 4425.

18 S. Braun, W. R. Salaneck, M. Fahlman, *Adv. Mater.* 2009, **21**, 1450.

19 T. Honda,T. Kojima, S. Fukuzumi, *Chem. Commun.* 2011, **47**, 7986.